

Three-dimensional inverse modelling of pneumatic tests in unsaturated fractured rocks

VELIMIR V. VESSELINOV, SHLOMO P. NEUMAN & WALTER A. ILLMAN

Department of Hydrology and Water Resources, The University of Arizona, Tucson, Arizona 85721-0011, USA

e-mail: monty@hwr.arizona.edu

Abstract A three-dimensional inverse model was used to analyse air pressure data from single- and cross-hole air injection tests in unsaturated fractured tuffs at the Apache Leap Research Site in Arizona. The model simulates single-phase airflow in a uniform, isotropic continuum. It treats open borehole intervals as high-permeability and high-porosity cylinders of finite length and radius. Single-hole test data yield local-scale permeabilities, porosities and borehole storage coefficients. Cross-hole test data yield larger-scale permeabilities, porosities and their spatial distributions.

INTRODUCTION

Over 270 single-hole (Guzman *et al.*, 1996; Guzman & Neuman, 1996), and over 40 cross-hole (Illman *et al.*, 1998) pneumatic injection tests have been conducted in 16 vertical and slanted boreholes (Fig. 1) completed within a layer of slightly welded, fractured, unsaturated tuff at the Apache Leap Research Site (ALRS) in Arizona. Steady state analyses of single-hole test data have been reported by Guzman *et al.* (1996), and transient type curve analyses of both single- and cross-hole test data by Illman *et al.* (1998). We describe numerical inversion of the test data by means of the finite volume code FEHM (Zyvoloski *et al.*, 1997), coupled with the inverse code PEST (Doherty *et al.*, 1994), using a multiprocessor supercomputer (SGI Origin 2000).

NUMERICAL INVERSE MODEL

Laboratory tests of core samples show that porous blocks of fractured tuff at the ALRS are virtually saturated with water. However, the void space of fractures at the site tends to be occupied primarily with air. It follows that air flow occurs primarily through fractures and can be simulated as single phase. Due to air compressibility, the corresponding airflow equations are nonlinear. Fractures at the site appear to form an interconnected three-dimensional network that we represent by a uniform and isotropic continuum. It follows that air permeabilities, and air-filled porosities, identified from pneumatic test data at the ALRS, reflect the bulk properties of fractures.

Paillet (1993) has noted that adding an observation borehole had an impact on drawdowns during an interference test in an aquifer. Preliminary simulations of cross-hole tests at the ALRS (Illman *et al.*, 1998) have shown that open borehole intervals have a considerable impact on pressure propagation through the system. We therefore

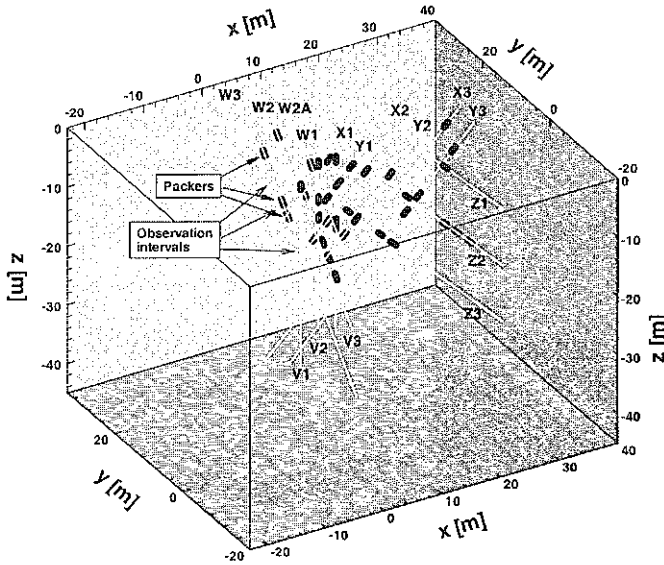


Fig. 1 Three-dimensional perspective of the site and computational region.

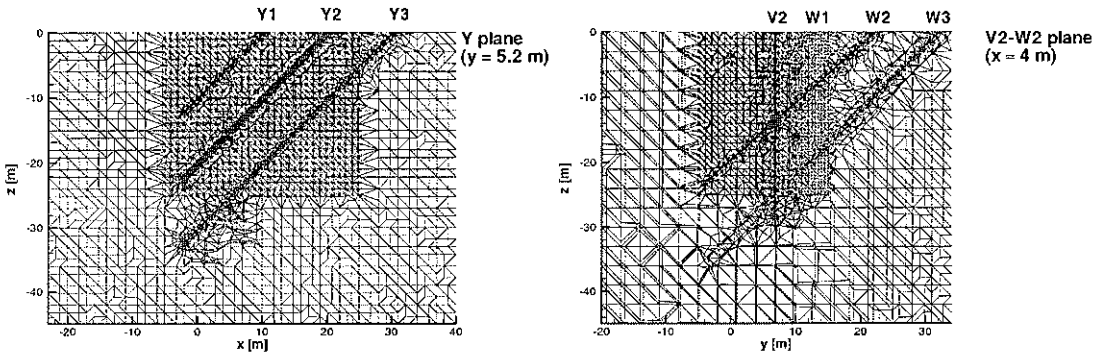


Fig. 2 Cross-sections through the computational grid (after Illman et al., 1998).

included such intervals in our model by treating them as high-permeability and high-porosity cylinders of finite length and radius.

The simulated flow region corresponds to the shaded rock volume in Fig. 1, which measures $153\,090\text{ m}^3$ ($63 \times 54 \times 45\text{ m}^3$). The side and bottom boundaries of the flow region are made to be impermeable; preliminary simulations (Illman et al., 1998) have suggested that these boundaries are sufficiently far from injection intervals to have virtually no effect on simulated pneumatic tests. The top boundary coincides with the ground surface and is maintained at a constant and uniform pressure of 0.1 MPa, corresponding to average barometric pressure during the tests. Though barometric pressure fluctuated during each pneumatic test, these fluctuations are ignored in our analysis. Initial air pressure in the rock is likewise set equal to 0.1 MPa. The pneumatic properties of the medium remain constant in time.

A three-dimensional computational grid of tetrahedral elements was generated automatically by means of the code X3D (Trease *et al.*, 1996). It consists of: a regular grid at the centre, with node spacing of 1 m; a surrounding regular grid with node spacing of 3 m; and a much finer and more complex unstructured grid surrounding each borehole. The grid associated with the injection borehole is wider and finer than those associated with other boreholes so as to allow accurate resolution of the relatively high pressure gradients that develop around the former. There is a gradual transition from fine borehole grids having radial structures and surrounding coarser grids having regular structures. Two cross-sectional views of a grid constructed for the case of injection into an interval along borehole Y2 are illustrated in Fig. 2. The grid includes 39 264 nodes and 228 035 tetrahedral elements. It allows resolving medium heterogeneity on a scale of 1 m.

We developed a series of pre- and post-processing codes to allow seamless transfer of data between FEHM and PEST. The latter relies on the Levenberg-Marquardt algorithm (Marquardt, 1963) to estimate parameters by minimizing a weighted sum of squared difference between simulated and measured pressures at selected grid nodes, at selected times. Assuming that measurements are mutually uncorrelated and estimation errors are Gaussian, PEST calculates 95% confidence limits for each parameter. As these assumptions do not apply to our case, we view the corresponding confidence limits merely as crude indicators of parameter reliability.

NUMERICAL INVERSION OF PNEUMATIC TEST DATA

To illustrate the numerical inversion of single-hole test data, we consider test JG0921 (Guzman *et al.*, 1996) conducted in borehole Y2 at two successive injection rates, 8.014×10^{-6} and $3.967 \times 10^{-5} \text{ kg s}^{-1}$. The corresponding pressure build-up and recovery data are presented in Fig. 3. To analyse single-hole test data, we treat the rock as having uniform air permeability and air-filled porosity values. In the case of test JG0921, we first analysed pressure data from the first injection step. When open borehole intervals are not included in the model (nodes along the axes of these intervals are assigned properties similar to those of the surrounding rock), the inverse model yields an air permeability k of $2.3 \times 10^{-14} \pm 2.6 \times 10^{-16} \text{ m}^2$ and an air-filled porosity ϕ of $4.5 \times 10^{-1} \pm 1.9 \times 10^{-3}$ (where the \pm range represents computed 95% linear confidence intervals). The latter porosity is much too high for fractures, and the corresponding pressure response (dashed curve in Fig. 3) does not match the observed pressures (dots for measured values, open circles for match points) well. When open borehole intervals are included (by assigning to them high permeability and porosity values), and the effective porosity ϕ_w of the injection interval is treated as an unknown parameter, the computed pressure (solid curve in Fig. 3) matches the observed values very well. The corresponding parameter estimates are $k = 2.2 \times 10^{-14} \pm 4.4 \times 10^{-16} \text{ m}^2$, $\phi = 6.7 \times 10^{-3} \pm 4.7 \times 10^{-3}$, and $\phi_w = 7.0 \times 10^{-1} \pm 6.7 \times 10^{-2}$. The relatively large confidence interval associated with ϕ reflects low reliability due to borehole storage effects at an early time. This adverse effect can be minimized by considering all available pressure data, especially those measured during recovery (Vesselinov & Neuman, 2000). The corresponding fit (Fig. 3) between computed (solid) and measured (dots and circles) data, obtained with $k = 2.4 \times 10^{-14} \pm 7.1 \times 10^{-16} \text{ m}^2$,

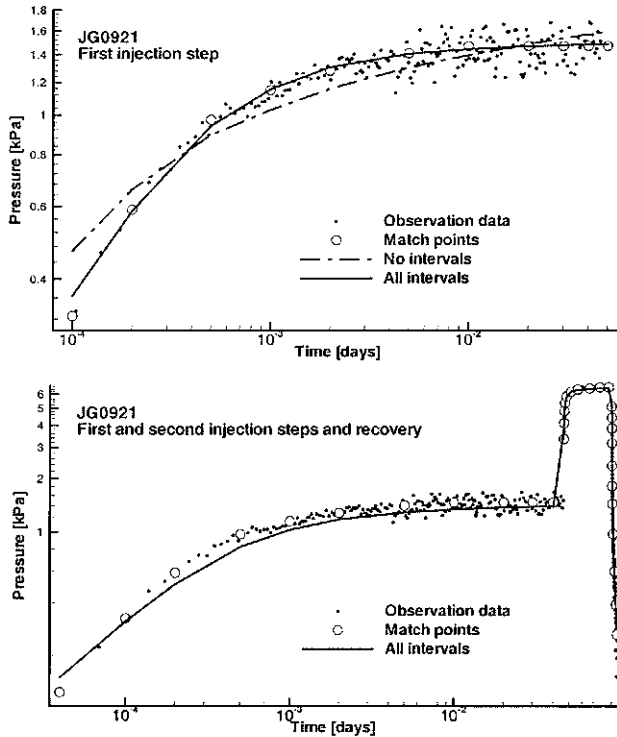


Fig. 3 Analysis of single-hole test data (after Vesselinov & Neuman, 2000).

$\phi = 1.4 \times 10^{-2} \pm 1.7 \times 10^{-3}$, and $\phi_w = 8.0 \times 10^{-1} \pm 4.6 \times 10^{-2}$, is good. The latter estimate of permeability is close to that obtained by means of steady state (Guzman *et al.*, 1996) and transient type curve (Illman *et al.*, 1998) analyses of the first step of the test. Unfortunately, these analyses did not yield unique values of porosity.

For illustration purposes we discuss the analysis of one cross-hole test labelled PP4 (Illman *et al.*, 1998). Air was injected into the middle (Y2-2) of three intervals along borehole Y2 at a rate of $1 \times 10^{-3} \text{ kg s}^{-1}$. The locations of packers during this test are shown in Fig. 1. The length of monitored intervals varies between 0.5 and 42.6 m; the distance from the injection interval to observation intervals ranges from 1.0 to 30 m. Though pressure responses were recorded in 32 of all 36 packed-off borehole intervals, we present only 12 of these pressure records in Fig. 4. We started by treating the medium as uniform and analysing each pressure record individually. The computed pressure is shown by solid curves in Fig. 4, which also lists the corresponding parameter estimates. Inverse permeability estimates are quite close to those obtained by means of type-curves (Illman *et al.*, 1998).

It is of interest to note that the injection intervals in cross-hole test PP4 and single-hole test JG0921 virtually coincide. Though the injection rate during PP4 had exceeded that during JG0921 by a factor of about 100, both tests yielded similar permeabilities and porosities for the injection interval.

To perform a simultaneous inverse analysis of pressure data from 32 of the monitored borehole intervals simultaneously, we allow air permeability to vary in space

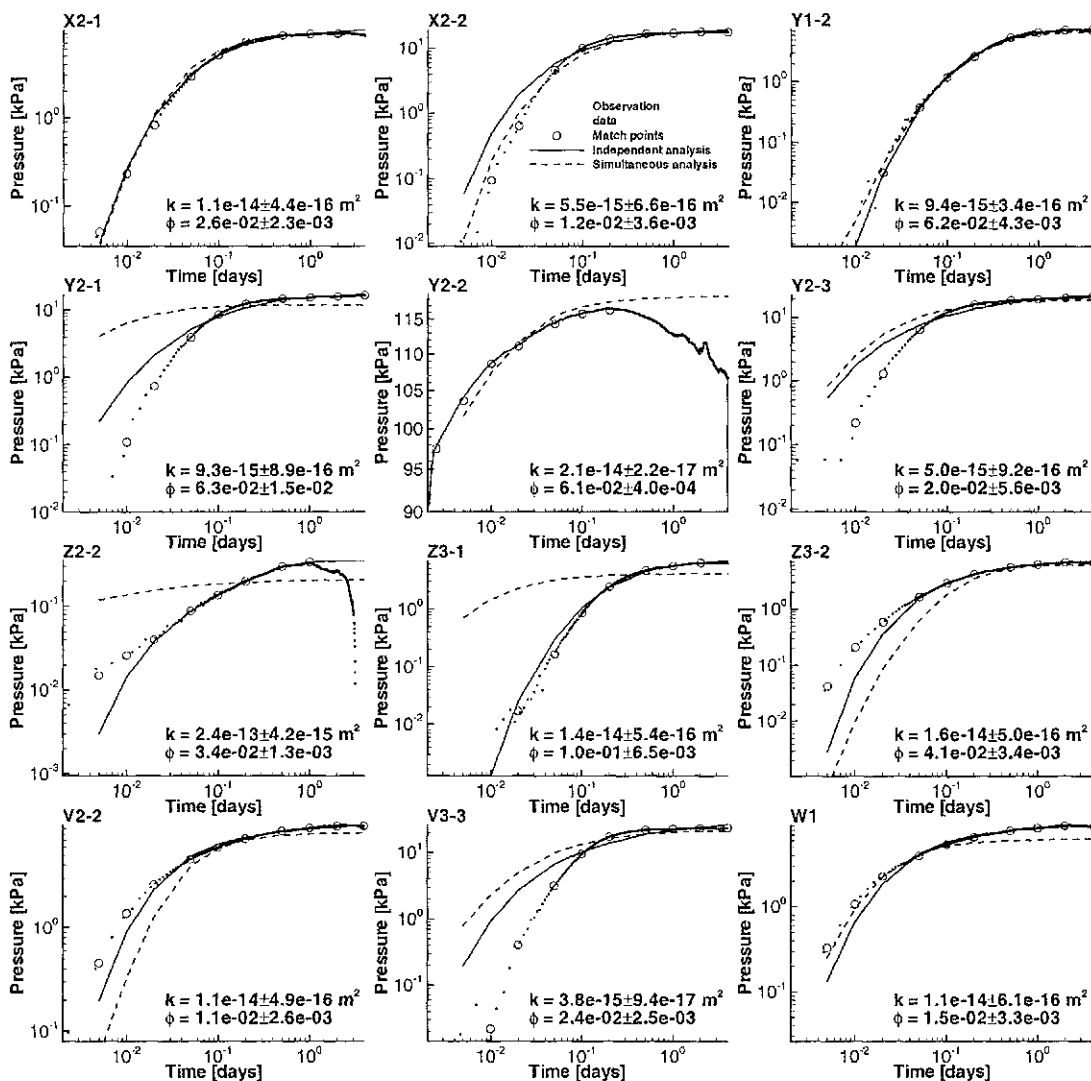


Fig. 4 Independent and simultaneous analyses of cross-hole test data. Parameter estimates are from independent analysis.

while treating porosity as an unknown constant. Log permeability is kriged based on 32 “measurement” or “pilot” points at which the corresponding “measured values” are treated as unknowns. The pilot points are located along the injection and various monitoring intervals. Kriging is performed by means of the geostatistical code GSTAT (Pebesma & Wesseling, 1998), using a power variogram with an unknown exponent that is not allowed to exceed 1. A cross-section through the estimated log permeability field (with an estimated variogram exponent of 1) is given in Fig. 5, and corresponding pressure build-ups are shown by dashed curves in Fig. 4. Some of the fits are better than those obtained by treating the rock as being uniform (solid curves), and some are worse. We expect to improve the fit in the future by allowing porosity to vary in space.

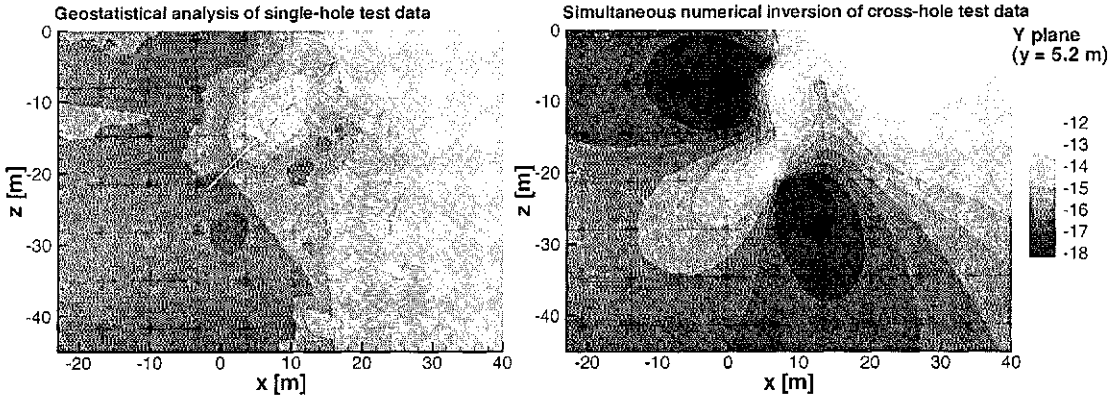


Fig. 5 Cross-sections through permeability ($\log_{10} k [m^2]$) fields, obtained by means of two different approaches.

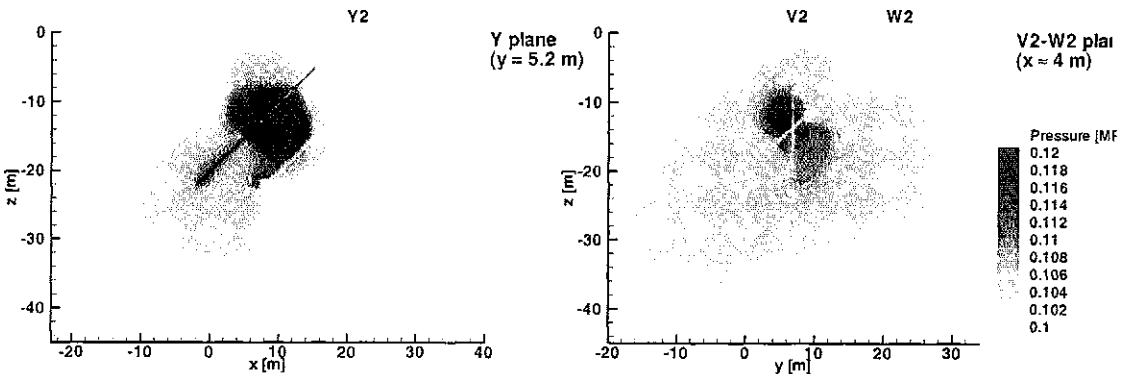


Fig. 6 Simulated spatial distributions of air pressure at end of cross-hole test PP4.

Kriging log permeability values obtained from single-hole tests (Illman *et al.*, 1998) leads to a different spatial distribution to that we had obtained by inverse analysis of cross-hole data (Fig. 5), but there are some important similarities. Attempts to use the kriged pattern of single-hole data as a basis for inverse analysis of cross-hole data have been unsuccessful.

Simulated air pressure distributions through the computational region at the end of cross-hole test PP4 are depicted in Fig. 6. The figure demonstrates the combined influence of heterogeneity and boreholes on airflow.

CONCLUSIONS

Pneumatic injection tests in unsaturated fractured tuffs are amenable to analysis by means of a three-dimensional numerical inverse model, which considers only single-phase airflow and treats the rock as a uniform, isotropic continuum representative of interconnected fractures. The inverse model accounts directly for the geometry,

conductance, and storage of open borehole intervals, which have an impact on the space-time pressure distribution in the system. It is possible to analyse pressure data from individual borehole intervals separately while treating air permeability and air-filled porosity as uniform, and from all intervals simultaneously by allowing permeability to vary in space. We hope to improve our analysis in the future by including spatial variations in air-filled porosity; heterogeneity of air-filled porosity will impact early time pressures. We are also planning to analyse simultaneously several cross-hole tests as well as a set of single-hole tests conducted along one borehole. Such analyses would amount to a hydraulic version of geophysical tomography, an idea proposed over a decade ago by Neuman (1987, p. 547).

Acknowledgements This work was supported by the US Nuclear Regulatory Commission under contracts NRC-04-95-038 and NRC-04-97-056. Velimir V. Vesselinov conducted part of the inverse modelling work during a summer internship at the Geoanalysis Group, Los Alamos National Laboratory. We are grateful to George A. Zyvoloski for his help in the implementation of FEHM, and to Carl W. Gable for his assistance in the use of X3D.

REFERENCES

- Doherty, J., Brebber, L. & Whyte, P. (1994) *PEST: Model Independent Parameter Estimation*. Watermark Computing, Brisbane, Australia.
- Guzman, A. G., Neuman, S. P. (1996) Field air injection experiments. In: Apache Leap Tuff INTERVAL Experiments (ed. by T. Rasmussen, S. C. Rhodes, A. G. Guzman & S. P. Neuman), 52–94. *Tech. Report NUREG/CR-6096, US Nuclear Regulatory Commission*.
- Guzman, A. G., Geddis, A. M., Henrich, M. J., Lohrstofer, C. F. & Neuman, S. P. (1996) Summary of air permeability data from single-hole injection test in unsaturated fractured tuff at the Apache Leap Research Site: results of steady-state test interpretation. *Tech. Report NUREG/CR-6360, US Nuclear Regulatory Commission*.
- Illman, W. A., Thompson, D. L., Vesselinov, V. V., Chen, G. & Neuman, S. P. (1998) Single- and cross-hole pneumatic tests in unsaturated fractured tuffs at the Apache Leap Research Site: Phenomenology, spatial variability, connectivity and scale. *Tech. Report NUREG/CR-5559, US Nuclear Regulatory Commission*.
- Marquardt, D. W. (1963) An algorithm for least-squares estimation of nonlinear parameters. *J. Soc. Industr. Appl. Math.* **11**, 431–441.
- Neuman, S. P. (1987) Stochastic continuum representation of fractured rock permeability as an alternative to the REV and fracture network concepts. In: *Rock Mechanics* (ed. by I. W. Farmer, J. J. K. Daemen, C. S. Desai, C. E. Glass & S. P. Neuman) (Proc. 28th US Rock Mechanics Symposium, Boston), 533–561. A. A. Balkema, Rotterdam, The Netherlands.
- Paillet, F. L. (1993) Using borehole geophysics and cross-borehole flow testing to define connections between fracture zones in bedrock aquifers. *J. Appl. Geophys.* **30**, 261–279.
- Pebesma, E. J. & Wesseling, C. G. (1998) GSTAT: A program for geostatistical modelling, prediction and simulation. *Computers & Geosci.* **24**(1), 17–31.
- Trease, H. E., George, D., Gable, C. W., Fowler, J., Kuprat, A. & Khamyaseh, A. (1996) The X3D grid generation system. In: *Numerical Grid Generation in Computational Fluid Dynamics and Related Fields* (ed. by B. K. Soni, J. F. Thompson, H. Hauser & P. R. Eiseman). Engineering Research Center, Mississippi State Univ. Press, Mississippi, USA.
- Vesselinov, V. V. & Neuman, S. P. (2000) Numerical inverse interpretation of multistep transient single-hole pneumatic tests in unsaturated fractured tuffs at the Apache Leap Research Site. In: *Theory, Modeling and Field Investigation in Hydrogeology: A Special Volume in Honor of Shlomo P. Neuman's 60th birthday* (ed. by D. Zhang & C. L. Winter) Geological Society of America, Boulder, Colorado, USA.
- Zyvoloski, G. A., Robinson, B. A., Dash, Z. V. & Trease, L. L. (1997) Summary of the models and methods for the FEHM application. *Tech. Report LA-13307-MS, Los Alamos National Laboratory, USA*.